Characterization of two-photon polarization mixed states generated from entangled-classical hybrid photon source

H. Kumano,[1,2,*] **K. Matsuda,**[1] **S. Ekuni,**[1] **H. Sasakura,**[1,2] **and I. Suemune**[1,2]

[1]*Research Institute for Electronic Science, Hokkaido University, Sapporo 001-0021, Japan*
[2]*CREST, Japan Science and Technology Agency, Kawaguchi 332-0012, Japan*
[*]*kumano@es.hokudai.ac.jp*

Abstract: We experimentally prepare bi-photon mixed states in polarization employing an entangled-classical hybrid photon emitter which can properly model solid-state entangled photon sources with uncorrelated background photons. Polarization-uncorrelated photon pairs in totally mixed (TM) states are embodied with classical thermal radiation, while the polarization-entangled ones in a Bell state are generated by conventional parametric down conversion. The bi-photon states generated from the hybrid photon emitter are characterized in terms of a linear entropy–tangle plane, which reveals the formation of two-qubit Werner states. We also propose a direct way for evaluating the Werner states by means of minimal coincidence counts measurements. This simple method can be widely applicable in examining the bi-photon states from solid-state entangled photon sources, in which the polarization-entangled photon pairs have temporal correlation while the background photons in the TM states do not.

OCIS codes: (270.0270) Quantum optics; (270.5290) Photon statistics; (270.5585) Quantum information and processing; (230.5590) Quantum-well, -wire and -dot devices.

References and links

1. M. A. Nielsen and I. L. Chuang, *Quantum Computation and Qnautum Information* (Cambridge University Press, 2000).
2. A. K. Ekert, "Quantum cryptography based on Bell's theorem," Phys. Rev. Lett. **67**, 661–663 (1991).
3. C. H. Bennett, G. Brassard, C. Crépeau, R. Jozsa, A. Peres, and W. K. Wootters, "Teleporting an unknown quantum state via dual classical and Einstein-Podolsky-Rosen channels," Phys. Rev. Lett. **70**, 1895–1899 (1993).
4. D. Bouwmeester, J.-W. Pan, K. Mattle, M. Eibl, H. Weinfurter, and A. Zeilinger, "Experimental quantum teleportation," Nature **390**, 575–579 (1997).
5. P. W. Shor, "Scheme for reducing decoherence in quantum computer memory," Phys. Rev. A **52**, R2493–R2496 (1995).
6. C. H. Bennett, D. P. DiVincenzo, J. A. Smolin, and W. K. Wootters, "Mixed-state entanglement and quantum error correction," Phys. Rev. A **54**, 3824–3851 (1996).
7. P. Michler, *Single Semiconductor Quantum Dots* (Springer, 2009).
8. H. Kumano, S. Kimura, M. Endo, H. Sasakura, S. Adachi, S. Muto, and I. Suemune, "Deterministic single-photon and polarization-correlated photon pair generations from a single InAlAs quantum dot," J. Nanoelectron. Optoelectron. **1**, 39–51 (2006).
9. Y. Hayashi, K. Tanaka, T. Akazaki, M. Jo, H. Kumano, and I. Suemune, "Superconductor-based light emitting diode: demonstration of role of cooper pairs in radiative recombination processes," Appl. Phys. Express **1**, 1–3 (2008).
10. Y. Asano, I. Suemune, H. Takayanagi, and E. Hanamura, "Luminescence of a Cooper pair," Phys. Rev. Lett. **103**, 187001 (2009).

#147728 - $15.00 USD Received 18 May 2011; revised 9 Jun 2011; accepted 22 Jun 2011; published 11 Jul 2011

11. R. M. Stevenson, R. J. Young, P. Atkinson, K. Cooper, D. A. Ritchie, and A. J. Shields, "A semiconductor source of triggered entangled photon pairs," Nature **439**, 179–182 (2006).
12. N. Akopian, N. H. Lindner, E. Poem, Y. Berlatzky, J. Avron, D. Gershoni, B. D. Gerardot, and P. M. Petroff, "Entangled photon pairs from semiconductor quantum dots," Phys. Rev. Lett. **96**, 130501 (2006).
13. R. Hafenbrak, S. M. Ulrich, P. Michler, L. Wang, A. Rastelli, and O. G. Schmidt, "Triggered polarization-entangled photon pairs from a single quantum dot up to 30 K," New J. Phys. **9**, 315 (2007).
14. A. Mohan, M. Felici, P. Gallo, B. Dwir, A. Rudra, J. Faist, and E. Kapon, "Polarization-entangled photons produced with high-symmetry site-controlled quantum dots," Nat. Photonics **4**, 302–306 (2010).
15. R. F. Werner, "Quantum states with Einstein-Podolsky-Rosen correlations admitting a hidden-variable model," Phys. Rev. A **40**, 4277–4281 (1989).
16. W. J. Munro, D. F. V. James, A. G. White, and P. G. Kwiat, "Maximizing the entanglement of two mixed qubits," Phys. Rev. A **64**, 030302(R) (2001).
17. M. Caminati, F. De Martini, R. Perris, F. Sciarrino, and V. Secondi, "Nonseparable Werner states in spontaneous parametric down-conversion," Phys. Rev. A **73**, 032312 (2006).
18. G. Puentes, A. Aiello, D. Voigt, and J. P. Woerdman, "Entangled mixed-state generation by twin-photon scattering," Phys. Rev. A **75**, 032319 (2007).
19. Y.-S. Zhang, Y.-F. Huang, C.-F. Li, and G.-C. Guo, "Experimental preparation of the Werner state via spontaneous parametric down-conversion," Phys. Rev. A **66**, 062315 (2002).
20. M. Barbieri, F. De Martini, G. Di Nepi, P. Mataloni, G. M. D'Ariano, and C. Macchiavello, "Detection of entanglement with polarized photons: experimental realization of an entanglement witness," Phys. Rev. Lett. **91**, 227901 (2003).
21. M. Barbieri, F. De Martini, G. Di Nepi, and P. Mataloni, "Generation and characterization of Werner states and maximally entangled mixed states by a universal source of entanglement," Phys. Rev. Lett. **92**, 177901 (2004).
22. C. Kurtsiefer, S. Mayer, P. Zarda, and H. Weinfurter, "Stable solid-state source of single photons," Phys. Rev. Lett. **85**, 290–293 (2000).
23. P. Michler, A. Imamoğlu, M. D. Mason, P. J. Carson, G. F. Strouse, and S. K. Buratto, "Quantum correlation among photons from a single quantum dot at room temperature," Nature **406**, 968–970 (2000).
24. C. Santori, M. Pelton, G. Solomon, Y. Dale, and Y. Yamamoto, "Triggered single photons from a quantum dot," Phys. Rev. Lett. **86**, 1502–1505 (2001).
25. D. F. V. James, P. G. Kwiat, W. J. Munro, and A. G. White, "Measurement of qubits," Phys. Rev. A **64**, 052312 (2001).
26. P. G. Kwiat, K. Mattle, H. Weinfurter, A. Zeilinger, A. V. Sergienko, and Y. Shih, "New high-intensity source of polarization-entangled photon pairs," Phys. Rev. Lett. **75**, 4337–4341 (1995).
27. J. S. Bell, *Physics* (1965), Vol. 1, p. 165.
28. R. J. Young, R. M. Stevenson, A. J. Hudson, C. A. Nicoll, D. A. Ritchie, and A. J. Shields, "Bell-inequality violation with a triggered photon-pair source," Phys. Rev. Lett. **102**, 030406 (2009).
29. W. K. Wootters, "Entanglement of formation of an arbitrary state of two qubits," Phys. Rev. Lett. **80**, 2245–2248 (1998).
30. S. Bose and V. Vedral, "Mixedness and teleportation," Phys. Rev. A **61**, 040101(R) (2000).
31. C. Cinelli, G. Di Nepi, F. De Martini, M. Barbieri, and P. Mataloni, "Parametric source of two-photon states with a tunable degree of entanglement and mixing: experimental preparation of Werner states and maximally entangled mixed states," Phys. Rev. A **70**, 022321 (2004).
32. C. H. Bennett, G. Brassard, S. Popescu, B. Schumacher, J. A. Smolin, and W. K. Wootters, "Purification of noisy entanglement and faithful teleportation via noisy channels," Phys. Rev. Lett. **76**, 722–725 (1996).
33. J. F. Clauser, M. A. Horne, A. Shimony, and R. A. Holt, "Proposed experiment to test local hidden-variable theories," Phys. Rev. Lett. **23**, 880–884 (1969).
34. B. Lounis, H. A. Bechtela, D. Gerionc, P. Alivisatosc, and W. E. Moernera, "Photon antibunching in single CdSe/ZnS quantum dot fluorescence," Chem. Phys. Lett. **329**, 399–404 (2000).
35. R. Loudon, *The Quantum Theory of Light*, 3rd ed. (Oxford University Press, 2000), Chap. 6.

1. Introduction

Quantum entanglement plays a crucial role in the field of quantum information [1], which provides us by far powerful functions in comparison with its classical counterpart. Entanglement is inherently endowed with a nonlocal correlation between separate quantum systems, and is regarded as inevitable resources for most applications such as quantum key distribution [2], quantum teleportation [3, 4], and quantum error correction [5, 6], etc. Apparently, practical sources of entangled photon pairs are one of the most important elements to implement these functions. In view of synchronized operation to clock pulses in larger systems, on-demand operation is quite desirable. Thus, solid-state photon sources based on semiconductor quan-

#147728 - $15.00 USD Received 18 May 2011; revised 9 Jun 2011; accepted 22 Jun 2011; published 11 Jul 2011

tum dots (QDs) [7–10] are expected to play a dominant role as polarization-entangled photon sources. [11–14] Although the maximally entangled states (Bell states) are required to draw its full potential, practical solid-state photon sources emit statistical mixture of the Bell states and unavoidable polarization-uncorrelated photons in totally mixed (TM) states which stem from surrounding environments. Therefore, in examining polarization-entangled photon states generated from realistic solid-state sources, Werner state [15, 16] as a linear combination of the Bell states and the TM states is of great significance as a bi-photon state deviated from the ideal Bell state. The Werner states have also manageable features that they are robust against nonlocal loss [17] and scatterings [18] which are likely to take place in solid-state media.

In general, the polarization-entangled photon pairs possess temporal correlation in the form of simultaneous twin-photon generation for parametric down conversion (PDC) sources or cascaded photon-pair emission [8] for the solid-state QD sources. On the other hand, temporal correlation between photon pairs in the TM states depends on the sources. So far, TM states obtained by polarization-decohered PDC sources have been reported [18–21] to prepare the Werner states. After a decoherer, the polarization correlation between generated twin-photons is lost but the temporal correlation remains. In the case of solid-state sources, however, background photons in the TM state originate from defects and imperfections, which independently work as sub-poissonian photon sources [22]. Then the bi-photon states involve different excitation events and inherently have no temporal correlation, as indicated by second-order photon correlation function of unity [23, 24]. Therefore, from a viewpoint of temporal correlation, the Werner states originated from the solid-state sources are not identical to the ones prepared with the polarization-decohered TM states.

In this paper, we experimentally prepare the Werner states employing entangled and classical hybrid photon-sources. An incoherent thermal radiation source is used for generating classical photons in which both the polarization and temporal correlations are absent. This will reproduce the nature of background photons generated from solid-state entangled photon sources. The heterogeneous nature in the temporal correlation between photon pairs from the entangled and classical sources make it possible to decompose an experimentally obtained coincidence counts histogram into the constituent photon-sources' contribution. This allows us to directly evaluate the photon-pair states in the Werner states by minimal coincidence counts measurements without reconstructing density matrix [25]. This will be highly beneficial for examining the polarization-entangled bi-photon states generated from the solid-state sources including temporally correlated background photons.

2. Experimental

Figure 1 shows a schematic of our experimental setup. The pump source is a 401 nm cw laser diode (Nichia NDV4313) with a typical output power of 90 mW at 95 mA driving current. A 2-mm-thick β-BaB_2O_4 (BBO) crystal, cut for type-II phase matching at $\theta = 42.3^\circ$ is used for generating PDC photon pairs with their central wavelength of 802 nm in non-collinear configuration. For degenerated photon-pair emission, the intersection lines of the emission cones form an angle of 6° and the tangents in the crossing points are perpendicular to each other, which is adjusted with an aid of a CCD image sensor (Watec, minimum illumination: 0.00002 lx. F1.4). The down converted photons pass through a half-wave plate (HWP) and additional BBO crystals with a thickness of 1 mm to compensate the transverse and longitudinal walk-off [26] introduced by the birefringence of the conversion crystal. For a classical thermal radiation source, a halogen bulb (Philips FocusLine) is employed, which can properly mimic the correlation-less and incoherent features of background emission from solid-state sources. The density matrix for the bi-photon polarization state is measured by a quantum-state tomography under 16 polarization configurations [25] prepared with quarter-wave plates, HWPs, and Glan-

#147728 - $15.00 USD Received 18 May 2011; revised 9 Jun 2011; accepted 22 Jun 2011; published 11 Jul 2011

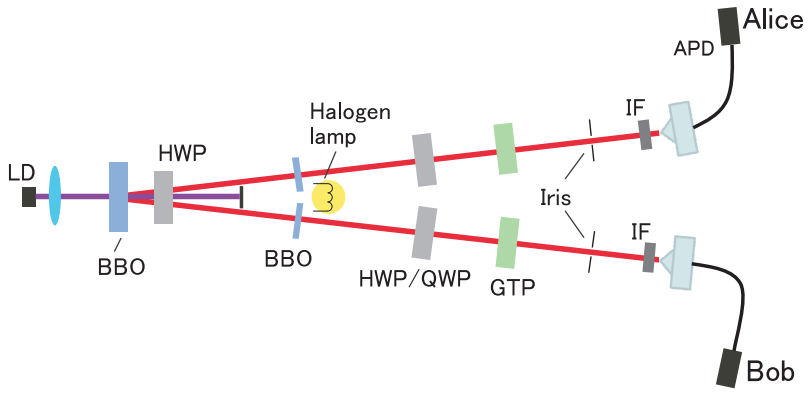

Fig. 1. A schematic of experimental configurations used in this work. As an polarization- and temporally-uncorrelated photon source, thermal radiation source (Halogen lamp) is employed. The Bell states are generated by the conventional PDC process. This entangled-classical hybrid photon-source forms the bi-photon Werner state, which will appropriately model solid-state polarization-entangled photon sources including temporally uncorrelated background photons.

Thompson linear polarizers. In order to precisely define the spatial mode, small irises (typical diameter is 1.5 mm) are introduced in each arm (Alice and Bob). A pair of 5-nm-band width interference filter (IF) centered at 800 nm (FUJITOK Corporation) is placed in front of silicon avalanche photodiodes (EG&G, SPCM-AQR) to limit the bandwidth of the incident photons and also to reduce background counts. The detector outputs are transferred to ratemeters for monitoring single count rates in each arm as well as to a time-to-amplitude converter followed by a multi-channel analyzer (MCA) in order to build up a coincidence counts histogram as a function of delay time. The time window for integrating the histogram is $4\sigma \sim 2.4$ ns as illustrated in Fig. 2(c), where σ gives a standard deviation of gaussian-distributed histogram. This 4σ time window covers 99.5% of the whole coincidence counts of the PDC photon pairs.

3. Evaluation of photon states from constituent emitters

Prior to mixing the PDC and thermal radiation sources, photon-pair states from the PDC and thermal radiation sources were separately evaluated. Bell's inequality test [27] was carried out for the PDC photon-pairs, and the Bell's S parameter measured with the standard linear-diagonal basis [28] was 2.552 ± 0.014, violating a Clauser-Horne-Shimony-Holt (CHSH) inequality with 39 standard deviation. The real and imaginary parts of the density matrix measured with the quantum-state tomography are displayed in Figs. 2(a) and 2(b), respectively.

Fidelity to the ideal singlet state

$$\rho_{Bell} = \left|\Psi^-\right\rangle\left\langle\Psi^-\right| = \begin{pmatrix} 0 & 0 & 0 & 0 \\ 0 & 1/2 & -1/2 & 0 \\ 0 & -1/2 & 1/2 & 0 \\ 0 & 0 & 0 & 0 \end{pmatrix}, \tag{1}$$

where $\left|\Psi^-\right\rangle = \frac{1}{\sqrt{2}}(|HV\rangle - |VH\rangle)$ is one of the Bell states, reached to 0.94. In order to discuss the formation and determination of the Werner states, measured bi-photon states were investigated from the viewpoint of degree of entanglement and mixedness by using tangle (T) [29] and linear

#147728 - $15.00 USD Received 18 May 2011; revised 9 Jun 2011; accepted 22 Jun 2011; published 11 Jul 2011

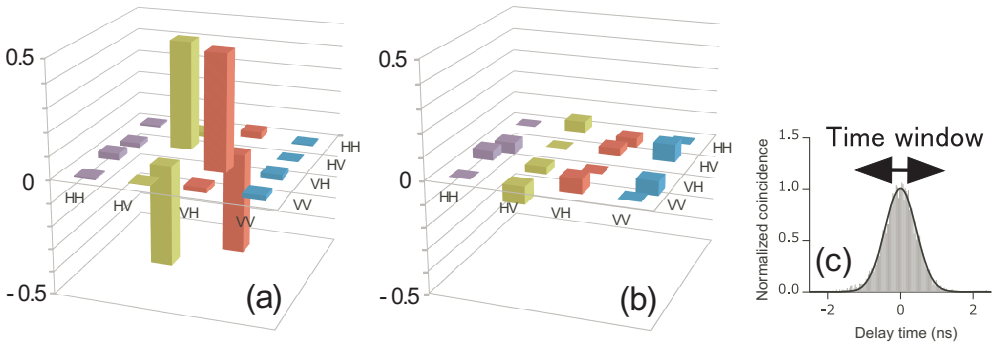

Fig. 2. Real (a) and imaginary (b) part of the density matrix for the photon-pair state from the PDC process measured with quantum-state tomography in the bases of $|HH\rangle, |HV\rangle, |VH\rangle$, and $|VV\rangle$. Fidelity to the state $\rho_{Bell} = |\Psi^-\rangle\langle\Psi^-|$ reaches to 0.94. (c) Typical coincidence counts histogram build up by the MCA. Solid curve is a fitted result with a Gaussian function $\exp[-(\tau/\sigma)^2]$, where τ is the delay time and $\sigma = 0.611$ ns. Time window for integrating the histogram was set to 4σ as indicated by an arrow, which gives $\int_{-2\sigma}^{2\sigma} \exp[-(\tau/\sigma)^2]d\tau \Big/ \int_{-\infty}^{\infty} \exp[-(\tau/\sigma)^2]d\tau = 0.995$.

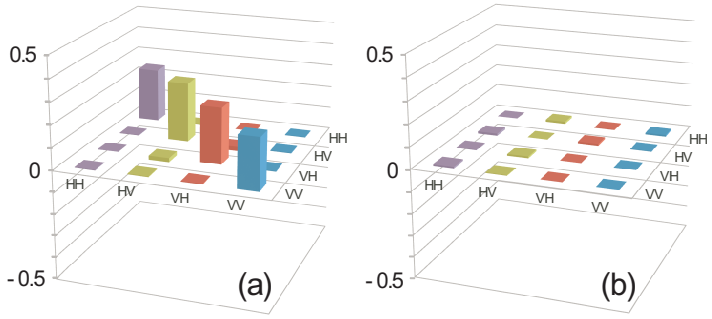

Fig. 3. Real (a) and imaginary (b) part of the measured density matrix for the thermal radiation source. The real diagonal elements are almost the same in amplitude of $\sim 1/4$, and the nondiagonal elements are ignorable. Fidelity to the state totally mixed state $\rho_{TM} = \frac{1}{4} I \otimes I$ is as high as 0.99.

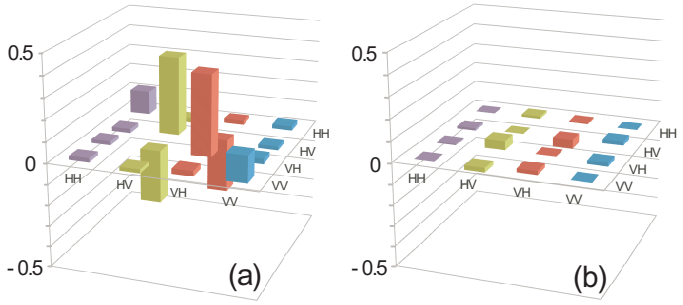

Fig. 4. Real (a) and imaginary (b) part of the measured density matrix for the hybrid photon source. Single photon count rates for the thermal and PDC sources are 2,700 and 40,000 s^{-1}, respectively.

#147728 - $15.00 USD Received 18 May 2011; revised 9 Jun 2011; accepted 22 Jun 2011; published 11 Jul 2011

entropy (S_L) [30], respectively. These measures can be calculated explicitly from the measured density matrix in the standard bases of $|HH\rangle, |HV\rangle, |VH\rangle, |VV\rangle$ as [29, 30]

$$T = [\max(\lambda_1 - \lambda_2 - \lambda_3 - \lambda_4, 0)]^2, \tag{2}$$

$$S_L = \frac{4}{3}\left(1 - \mathrm{Tr}\rho^2\right), \tag{3}$$

where ρ is the measured density matrix, λ_i (i=1, 2, 3, 4) is the square root of the eigenvalues in decreasing order of magnitude of the spin-flipped density matrix operator $R = \rho(\sigma^y \otimes \sigma^y)\rho^*(\sigma^y \otimes \sigma^y)$, where σ^y is one of the Pauli's operators, and the asterisk indicates complex conjugation. The tangle is zero for unentangled states and 1 for completely entangled states, while the linear entropy is zero for pure states and 1 for TM states.

On the other hand, density matrix for photon states measured from the thermal radiation source is shown in Fig. 3. Due to the lack of polarization correlation between photon pairs, real diagonal elements are equally balanced in amplitude and all the non-diagonal elements are vanished. Fidelity to the TM state

$$\rho_{TM} = \frac{1}{4} I \otimes I = \begin{pmatrix} 1/4 & 0 & 0 & 0 \\ 0 & 1/4 & 0 & 0 \\ 0 & 0 & 1/4 & 0 \\ 0 & 0 & 0 & 1/4 \end{pmatrix} \tag{4}$$

reaches to as high as 0.99, where I is the identity operator of a single qubit. Therefore, the thermal radiation is shown to be a model photon-pair source in the totally mixed polarization states, which can be an alternative to the so-far reported classical photon-pair sources based on the decohered Bell states [18–21].

4. Werner state formation with the entangled-classical hybrid photon source and its temporal correlation

Polarization-entangled photon-pair states generated from practical solid-state sources include finite contribution of uncorrelated background photons in TM states in addition to ideal polarization entangled photon pairs in Bell states. Therefore, the bi-photon states from the solid-state sources can be regarded as a convex combination of these two fundamental states in terms of polarization correlation, which yields a two-qubit Werner state described as

$$\rho_w = p\rho_{Bell} + (1-p)\rho_{TM} = p\left|\Psi^-\right\rangle\left\langle\Psi^-\right| + \frac{1-p}{4} I \otimes I, \tag{5}$$

where p is a singlet weight and ρ_{Bell} (ρ_{TM}) is a density matrix of the Bell (TM) state. In order to characterize bi-photon states from the entangled-classical hybrid photon emitter in which the identical temporal correlation with the solid-state sources is embodied, a series of bi-photon states were prepared in a way that single-photon count rates in each arm measured from the PDC source was fixed at 2,700 s^{-1} and only those from the thermal radiation were varied as (i) 0, (ii) 10,000, (iii) 15,000, (iv) 30,000, (v) 40,000, and (vi) 70,000 s^{-1}. As an example, experimentally obtained density matrix for the condition (v) is given in Fig. 4. It can be recognized as a convex combination of the density matrices presented in Figs. 2 and 3.

The resultant photon-pair states are plotted in a S_L–T plane as shown in Fig. 5, in which the gray area corresponds to unphysical photon-pair states, and the solid curve indicates the Werner state given by Eq. (5). All the measured photon-pair states indicated by the solid circles coincide well with the Werner curve. This reveals that the present hybrid photon emitter works as

#147728 - $15.00 USD Received 18 May 2011; revised 9 Jun 2011; accepted 22 Jun 2011; published 11 Jul 2011

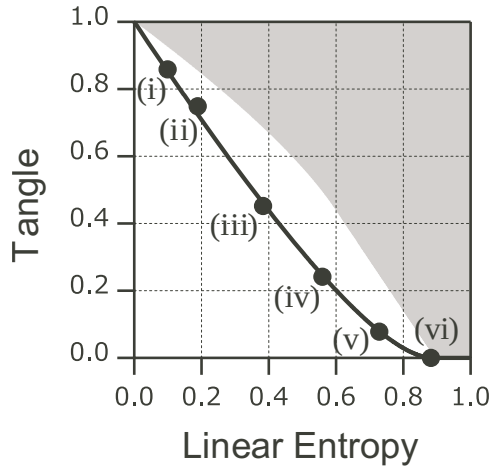

Fig. 5. Photon-pair states in the linear entropy (S_L)–Tangle (T) plane calculated from measured density matrix by quantum-state tomography. State (i) corresponds to a photon-pair state from the PDC source. States (ii) – (vi) exhibit photon-pair states originated form the PDC-classical hybrid photon source. Solid line indicates the Werner states, and the gray area corresponds to the states physically not realized. It can be seen that all the experimentally determined photon-pair states (solid circles) are well aligned on the Werner line. Thus, applying the criterion discussed in Sec. 4, it is shown that states (i)–(v) are entangled, and two states (i)–(iii) are also violating the CHSH inequality.

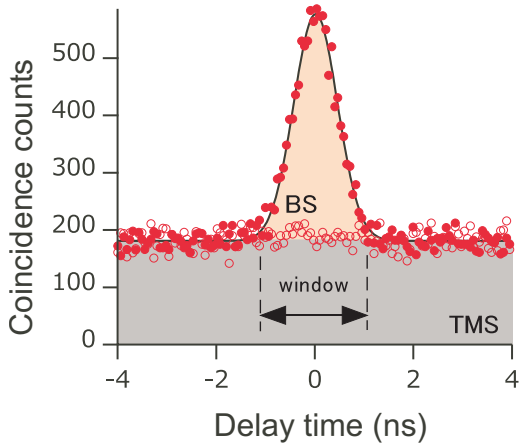

Fig. 6. Coincidence counts histogram built up in a MCA with HV (closed circles) and HH (open circles) detection polarizations for the bi-photon state (vi) in Fig. 5 and the fit result with a Gaussian function (solid curve). Integration time was 600 sec. The constant level (gray area, labeled as ”TMS”) originates from the thermal radiation source emitting temporally uncorrelated totally mixed polarization state, while the bunching (red area, labeled as ”BS”) from the Bell state generated from the PDC source. A series of measurements (i)–(vi) in Fig. 5 were carried out under fixed single count rate for the PDC source while the intensity of the thermal source was swept, and therefore only the constant level (gray area in this figure) are basically modified in each measurement. Time window of $4\sigma \sim 2.4$ ns used for integration is shown by an arrow. Contribution of each source to the coincidence histogram is unambiguously defined.

#147728 - $15.00 USD Received 18 May 2011; revised 9 Jun 2011; accepted 22 Jun 2011; published 11 Jul 2011

a photon-pair source in the Werner state. When restricting ourselves to the Werner states by substituting ρ_w for ρ, Eqs. (2) and (3) reduce to $T = \left[\max\left(\frac{3p-1}{2}, 0\right)\right]^2$ and $S_L = 1 - p^2$, respectively [31]. Thus, the singlet weight p is the only parameter to specify the Werner state, and $p > 1/3$ ($S_L < 8/9$) is required for the entangled nonseparable photon pair [21, 32], while $p > 1/\sqrt{2}$ ($S_L < 1/2$) for violating the CHSH inequality [33]. Notice that in the range of $1/3 < p < 1/\sqrt{2}$, the state is entangled but the CHSH inequality still holds. Based on the above arguments, photon-pair states (i)–(v) are entangled and (i)–(iii) are also violating the CHSH inequality, while the state (vi) is no longer entangled but now separable. Following the above argument, estimation of the singlet weight p is required in order to judge whether the produced Werner state is entangled or not. For this purpose, coincidence counts under at least eight projective measurements including two for normalization are normally required [20]. We alternatively present that p can be directly obtained from the minimal coincidence counts measurements when the temporal correlation is absent in the bi-photon state ρ_{TM}. When the detection polarization is set to HV, which gives the highest coincidence count for the incident Bell state $|\Psi^-\rangle$, the contribution of the state ρ_{Bell} from the PDC source to the coincidence count as a function of singlet weight p is given by $C^{(Bell)}(p) = p\langle HV|\rho_{Bell}|HV\rangle = p/2$. On the one hand, the contribution of ρ_{TM} from the thermal source is expressed as $C^{(TM)}(p) = (1-p)\langle HV|\rho_{TM}|HV\rangle = (1-p)/4$. Therefore, the areal ratio $C^{(Bell)}/C^{(TM)}$ for a given time window is expressed as $2p/(1-p)$. Then the singlet weight is directly obtained by

$$p = C^{(Bell)}/(C^{(Bell)} + 2C^{(TM)}). \tag{6}$$

In order to evaluate the singlet weight p from the experimentally obtained coincidence count histogram, it is obvious that clear discriminability between $C^{(Bell)}$ and $C^{(TM)}$ associated with each constituent photon sources is a prerequisite. In so-far prepared Werner states [18–21], both the Bell and TM states were generated by the PDC process that gives simultaneous bi-photon emission in the common nonlinear crystal. Then the photon pairs in these two states have the identical temporal correlation and the measured coincidence counts for the Werner states are the sum of two identical temporal distribution functions with different Bell- and TM-state's amplitudes, which is located at around zero time-delay. Therefore, one cannot decompose the measured coincidence count histogram into two subsets from each photon sources. On the other hand, in the present entangled-classical hybrid photon source, the absence of temporal correlation in the thermal radiation sources introduces the discriminability of the coincidence counts $C^{(Bell)}$ and $C^{(TM)}$, as discussed hereafter.

Figure 6 shows coincidence counts measured on the corresponding bi-photon state (vi) in Fig. 5 under the detections of polarization HH (open circles) and HV (closed circles). Since the relation $\langle HH|\rho_{Bell}|HH\rangle = 0$ holds, the state ρ_{Bell} has no contribution to the coincidence counts under the HH detection. Thus, the time-independent constant counts (gray area in Fig. 6) originate from the TM state. The contribution of the TM state to the histogram is invariant under detection polarization rotation and independent on the detection angle in another arm. On the other hand, the state ρ_{Bell} under the HV-polarization detection gives coincidence counts localized at around zero time-delay. As shown by the solid line, the overall coincidence counts in the HV detection agree well with the gaussian-shaped coincidence counts from the Bell states superposed on the constant base counts from the TM states, which clearly discriminate the contribution of the constituent sources.

In order to investigate the two constituent photon sources from a viewpoint of temporal correlation, single count rate dependence of the coincidence count is examined for both the PDC and the thermal radiation sources. As shown in Fig. 7, the PDC source exhibits linear relation to the single rate, while the thermal radiation shows quadratic one. This difference can be explained as follows:

#147728 - $15.00 USD Received 18 May 2011; revised 9 Jun 2011; accepted 22 Jun 2011; published 11 Jul 2011

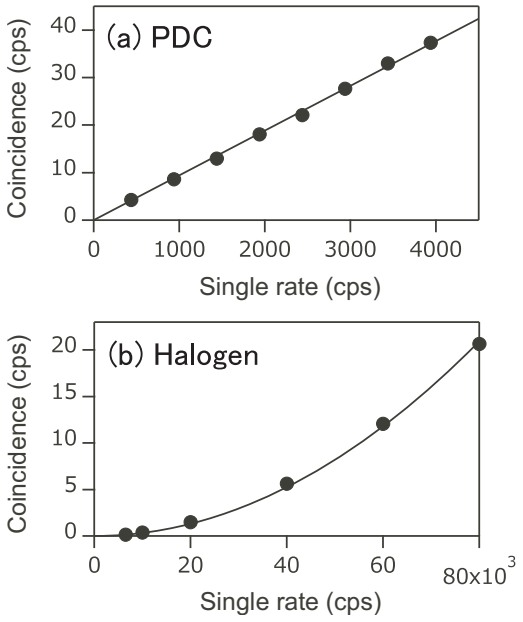

Fig. 7. Coincidence count as a function of single rate for the (a) PDC and (b) thermal sources. Detectors' dark counts are subtracted. The PDC source exhibits linear relation to the single rate due to the inherent temporal correlation between photons in a pair ($J^{(Bell)}(\tau) = \eta G(0,\sigma^2)$ with $\int_{-\infty}^{\infty} G(0,\sigma^2)d\tau = 1$), while the thermal source shows bilinear behavior because of the lack of temporal correlation and detection events of Alice and Bob are mutually independent ($J^{(TM)}(\tau) = R_{Bob}$) (see text). From the slope in the PDC, transmission coefficient for each arm is estimated to be ~ 1.0%.

Coincidence counts for Bell and TM states, i.e., the conditional probability of Bob's photon detection under the Alice's detection count rate of R_{Alice} is given by [34]

$$C^{(Bell/TM)} = \int_{-t_{win}/2}^{t_{win}/2} T_{acc}\, R_{Alice}\, J^{(Bell/TM)}(\tau)d\tau, \tag{7}$$

where t_{win} is the time window for integration, T_{acc} is the accumulation time, and $J^{(Bell)}(\tau)(J^{(TM)}(\tau))$ is the probability density detecting a photon in Bob's arm at time τ provided that there was a photon in Alice at time origin for the Bell (TM) state. For the PDC source, due to the simultaneous bi-photon generation, the probability density focuses on rather narrow time region at around $\tau = 0$ within a full time span of 50 ns in the MCA. Therefore, $J^{(Bell)}(\tau)$ can be expressed as $\eta G(0,\sigma^2)$, where η is the system transmission efficiency (including transmission of all optics as well as detection efficiency) and $G(0,\sigma^2)$ is a normalized Gaussian distribution function centered at $\tau = 0$ with a variance of σ^2. When the t_{win} is set so that $t_{win} \gg \sigma$, Eq. (7) reduces to $C^{(Bell)} = \eta\ T_{acc}\ R_{Alice}$. This explains the linear dependence observed in Fig. 7(a). Here the slope of ~ 0.01 corresponds to the system transmission η of our setup with $T_{acc} = 1$ ns. As for temporal distribution of the coincidence counts, since the $C^{(Bell)}$ does not include t_{win} with $t_{win} \gg \sigma$, coincidence counts are well localized at around the time origin as experimentally observed in Fig. 6. On the other hand, such temporal correlation is absent for the thermal radiation source. Thus the coincidence counts between photon-pair is regarded as an accidental event in the independent photon detection by Alice and Bob. Thus, through the relation $J^{(TM)}(\tau) = R_{Bob}$ and $R_{Alice} \approx R_{Bob}$, the quadratic relation $C^{(TM)} \sim t_{win} T_{acc}\, R_{Alice}^2$ holds as

#147728 - $15.00 USD Received 18 May 2011; revised 9 Jun 2011; accepted 22 Jun 2011; published 11 Jul 2011

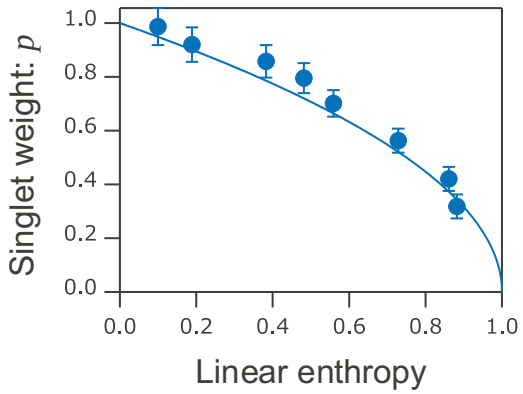

Fig. 8. Singlet weight p as a function of linear entropy obtained from Eq. (6). Solid line indicates calculated singlet weight as a function of S_L for the Werner state. The S_L values are common with Fig. 5.

observed in Fig. 7(b). The experimentally obtained quadratic coefficient is 3.27×10^{-9}, which agrees well to the expected value of $4\sigma \sim 2.4\times10^{-9}$. With respect to temporal distribution, $C^{(TM)}$ is now proportional to the t_{win}, then the coincidence count density is uniformly distributed over delay time as indicated by the gray area in Fig. 6.

Cross-term between the PDC and thermal sources could also give rise to the constant coincidence counts $C^{(cross)}$ since there is no temporal correlation between these independent photon sources. In the present case, however, $C^{(cross)}/C^{(Bell)}$ is estimated to be at most 3.5% for the bi-photon state (vi) in Fig. 5 with the highest intensity of the thermal radiation source. This is below the standard deviation of the amplitude of constant coincidence counts of ~ 7%, thus no significant difference in the constant coincidence amplitudes between the entangled-classical hybrid photon source and the thermal source alone was discerned under the present experimental conditions. Note that photon-pair states from the thermal radiation source leads to constant coincidence counts, and no effect of photon bunching for chaotic light [35] was detected. This is because the time resolution of our setup (~ 6.1 ps) is not enough to detect the bunching structure with a time scale of $\frac{\lambda_c^2}{c\delta\lambda} \sim 0.4$ ps, where c is the light velocity, λ_c is a center wavelength, and $\delta\lambda$ is a bandwidth of the IF filter.

5. Determination of the Werner states

Since the coincidence counts of $C^{(Bell)}$ and $C^{(TM)}$ are now independently obtained with the present entangled-classical hybrid photon emitter, we can evaluate the bi-photon Werner states from a single coincidence count histogram in principle. In case of Fig. 6, for example, the singlet weight p obtained from Eq. (6) is 0.32. This is highly close to the 0.34 calculated by the standard approach employing the density matrix built up by the quantum-state tomography for the same S_L assuming the Werner state.

In order to confirm the validity of this method, p values obtained from the Eq. (6) are compared with the ones obtained by the tomographically calculated values in Fig. 8. Uncertainties are also shown as error bars. The S_L values for each datapoints are common with Fig. 5, and the solid curve is a expected singlet weight as a function of the S_L for the Werner states. The obtained p values from the areal ratio in the coincidence histograms for each points are plotted as circles. Fairly nice agreement of p determined by the two separate measurements is achieved, thus the direct evaluation of the photon-pair states in the Werner state is shown to be possible.

#147728 - $15.00 USD Received 18 May 2011; revised 9 Jun 2011; accepted 22 Jun 2011; published 11 Jul 2011

The present method is rather instantaneous in the sense that p value can be speculated even in ongoing measurement from the Eq. (6) by glancing at building coincidence histogram and grasping $C^{(Bell)}$ and $C^{(TM)}$. Thus collecting whole data set and subsequent data processing to obtain full knowledge of the biphoton state is not required.

In conjunction with the expected robustness of the Werner state in the usual solid-state environment for photon-pairs, this simple method will be highly beneficial for examining polarization-entangled photon-pair states generated from the solid-state sources including the temporal-correlation-free background.

6. Conclusion

We have experimentally prepared the bi-photon Werner state in polarization employed with entangled-classical coupled photon sources. Heterogeneous nature of the temporal correlation in photon-pairs generated from the PDC and thermal radiation sources ensures the clear discriminability of each photon-pairs' contribution to the coincidence counts histogram. As a result, the generated bi-photon states in the Werner states can be directly evaluated with minimal coincidence counts measurements.

Acknowledgments

The authors would like to acknowledge Dr. H. Nakajima for fruitful discussions. This work was supported in part by the Grant-in-Aid for Scientific Research (A)(2), No.21246048, Young Scientists (A), No.21681020, and Inamori foundation.

#147728 - $15.00 USD Received 18 May 2011; revised 9 Jun 2011; accepted 22 Jun 2011; published 11 Jul 2011